Cell Tissue Kinet. (1988), **21**, 231–246.

Scoring mitotic activity in longitudinal sections of crypts of the small intestine

C. S. Potten, S. A. Roberts, S. Chwalinski, M. Loeffler* and U. Paulus*

*Paterson Institute for Cancer Research, Christie Hospital & Holt Radium Institute, Manchester M20 9BX, U.K. and *Medizinische Universitätsklinik, Joseph-Stelzmann Strasse 9, D5000 Köln 41, F.R.G.*

(*Received* 5 *July* 1987; *revision accepted* 1 *August* 1988)

Abstract. Various counts have been made of the number of mitotic figures in whole crypts and sections of crypts of the small intestine of the mouse. Samples were analysed from animals killed at different times of the day and at different times after administration of vincristine. Measurements have been made of the size of mitotic and interphase nuclei and of the radial position of mitotic figures. The correction factor, f, which is required to take into account the enhancement of mitotic counts in sections as a consequence of their centripetal position has been investigated. The results indicate the following: (1) transverse sections of the crypt differ from longitudinal sections if they involve cutting the intestine before fixation which may result in a relaxation of the crypt and its widening by 25%; (2) columnar cell nuclei have a shape that resembles a sphere flattened so that the average diameter is 20% greater in crypt transverse sections; (3) mitotic nuclei tend to be about half-way between the crypt edge and the central axis of the crypt; (4) between about four and seven times more mitotic figures have their mitotic axis parallel to the long axis of the crypt; (5) about one-third of all mitotic figures in a crypt are seen in a longitudinal section of the crypt. If this is related to the number of cells in the crypt as a whole and in a section, a correction factor f_D for the mitotic index of 0·59 is obtained; (6) the correction factor f_T derived from the shape and position of the mitotic figures measured in 3 μm longitudinal sections is 0·53; (7) relating cell cycle and mitotic accumulation data using a computer-based model of the crypt also permits a correction factor f_{mod} to be estimated. This gives a value of 0·66. When sectioned material is used to calculate a mitotic index the most appropriate correction factor is f_D; for mouse small intestine it is 0·59.

Cell proliferation in the crypts of the small intestine of experimental animals is often measured by recording either the absolute number, or the proportion, of mitotic figures. This can be conducted in sections — usually longitudinal with respect to the crypts, i.e. transverse with respect to the intestine — or in whole crypts isolated essentially as described by Wimber *et al.* (1960). The results can be expressed as an absolute number per crypt, or per crypt section, or as an index in which case the total number of non-mitotic cells has to be counted, of which probably only a proportion (poorly defined) are proliferating cells.

Correspondence: Dr C.S. Potten, Paterson Institute for Cancer Research, Christie Hospital & Holt Radium Institute, Wilmslow Road, Withington, Manchester M20 9BX, U.K.

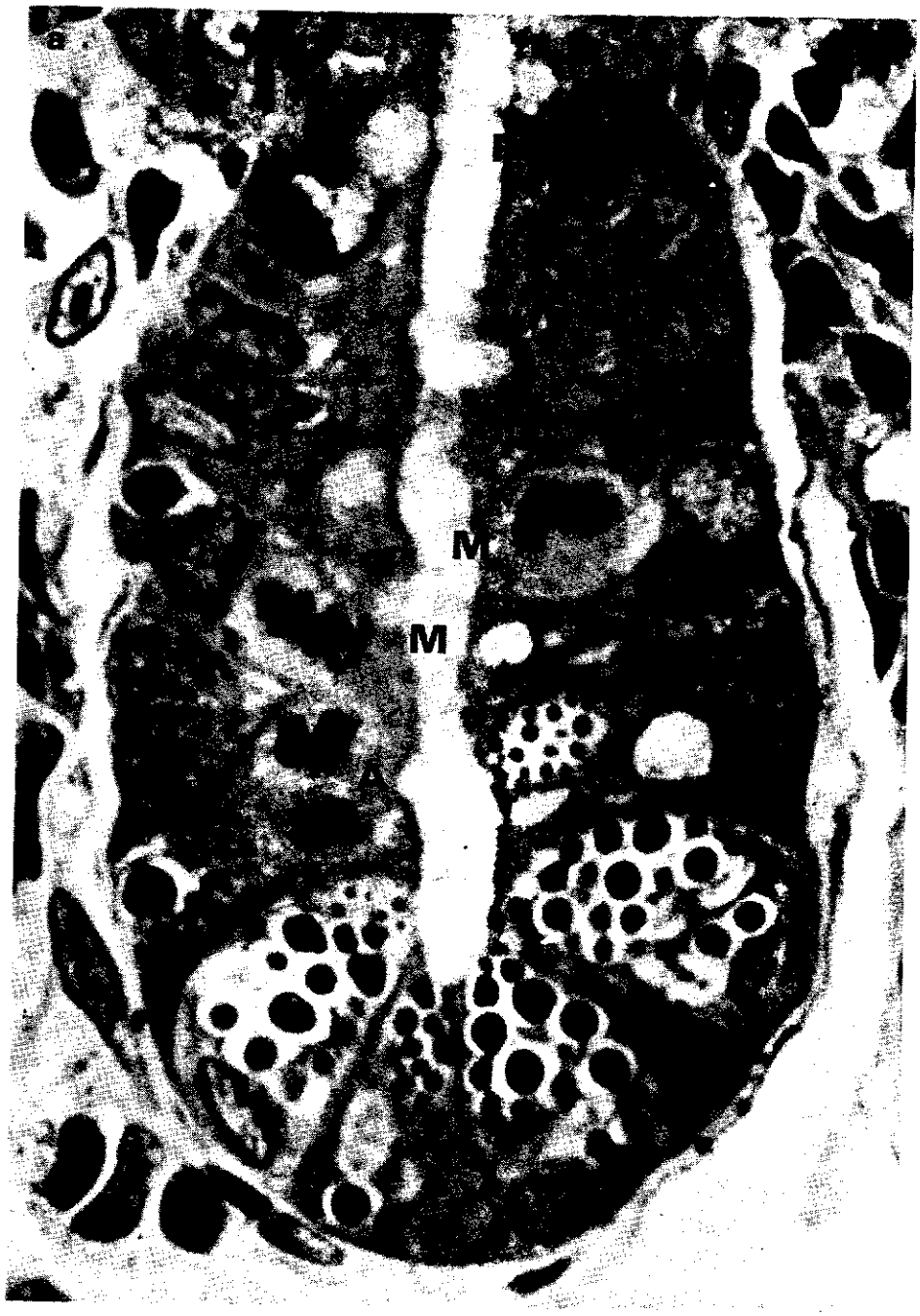

Fig. 1. Photomicrographs of 1 μm thick sections of resin-embedded small intestine stained with Masson's trichrome. (a) Longitudinal section of a crypt showing Paneth cells at the base and lumen of the crypt. Transverse sections of the crypt: (b) midcrypt, (c) near crypt base. Prophase (P), metaphase (M), anaphase (A). × 1750.

Mitotic cells in the crypts commonly have their chromatin material displaced towards the lumen of the crypt, i.e. their 'nuclei' are out of line with the remaining interphase crypt cell nuclei (see Figs 1 & 2). The reasons for this striking displacement of the nuclei are unknown but a similar process occurs in most columnar epithelia. Neither is it known how, or where relative to the other cells, the two daughter cells produced after division re-insinuate themselves

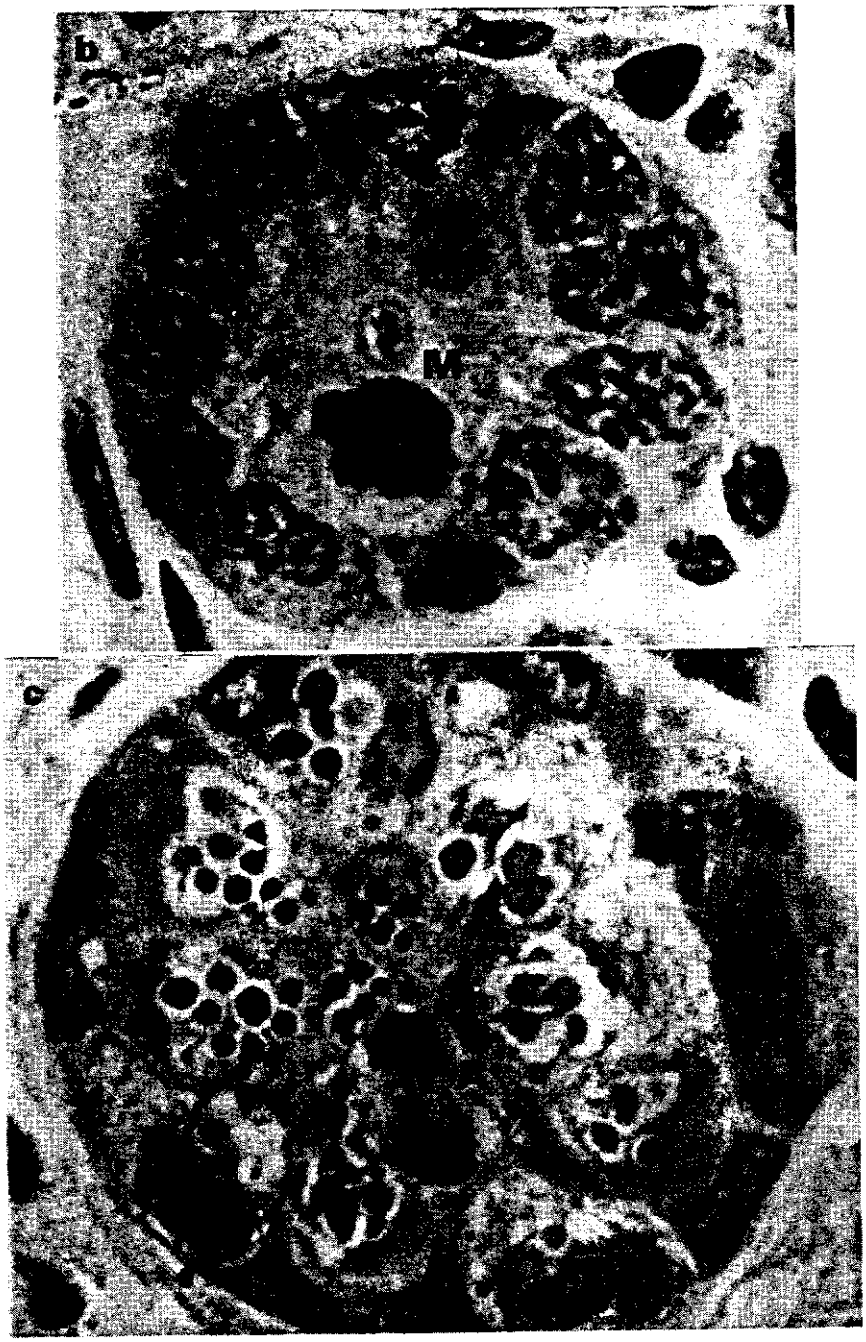

Fig. 1 *cont.*

but some speculations have been made (Lamprecht, Zieba & Strojng, 1986; Potten & Loeffler, 1987).

The centripetal displacement with respect to the crypts of the chromatin material in mitotic cells means that they will tend to appear in longitudinal sections relatively more frequently than they should when considered in relation to the peripheral interphase nuclei (see Fig. 3) because they have a greater chance of being sectioned. This results in an overestimate of their numbers as was recognized in 1967 by Tannock who suggested that a correction factor should be applied. This can be estimated by measuring the radial position of the mitotic figures in transverse sections of the crypts, the radius of the crypts and the diameter of mitotic figures in relation to

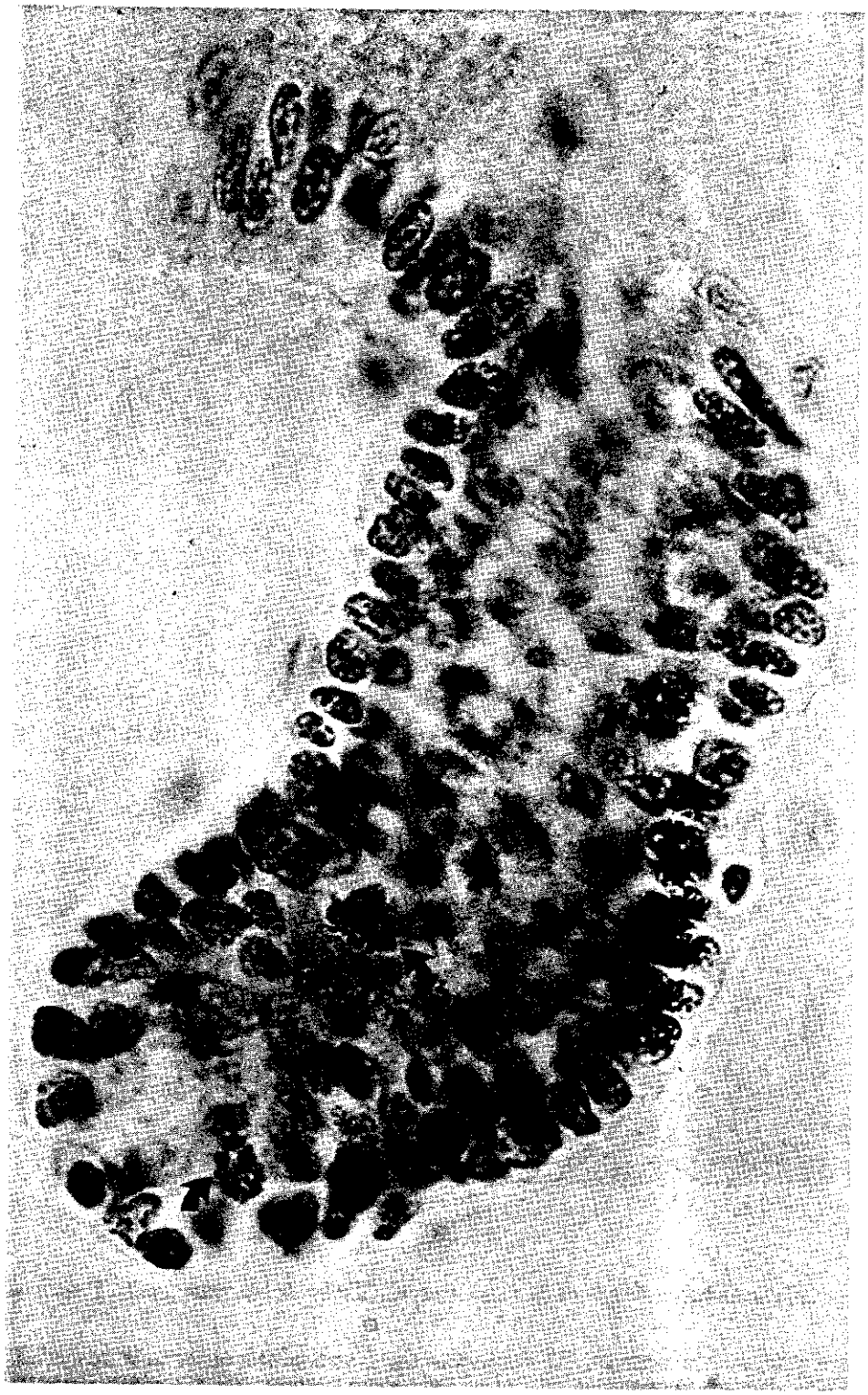

Fig. 2. Whole crypt after staining with Schiff's reagent. The microscope is focused to give an optical section through the middle of the crypt. Three mitotic figures can be clearly seen (arrows). × 850.

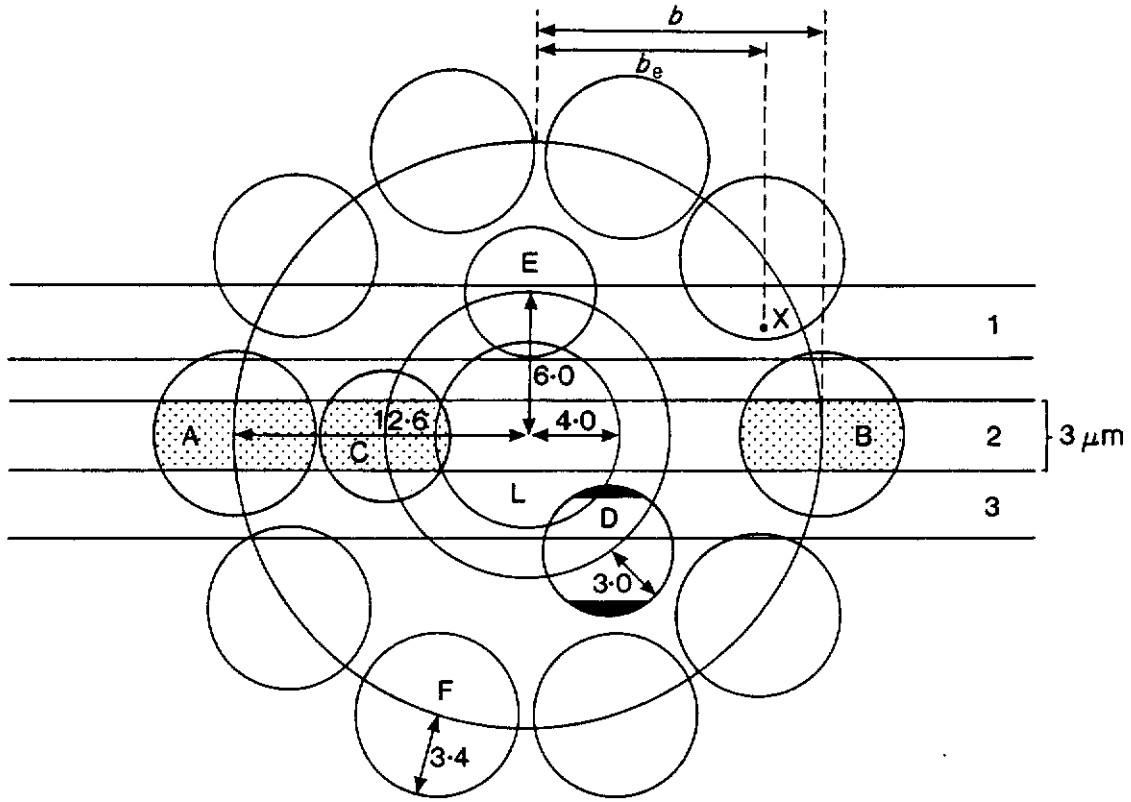

Fig. 3. Diagrammatic representation of a transverse section of a crypt showing 10 nuclei around the circumference. Various measurements have been made on such sections — the mean values obtained are shown on the diagram. Three representative 3 μm sections are shown each of which would probably satisfy the criteria for a good longitudinal section since they all include a section of the lumen (L). Two of the three sections would include interphase nuclei A and B. The central section (2) would include one mitotic figure (C) but section 3 would have two mitotic figures (C and D). Section 1 shows how the true crypt radius (b) will be underestimated in some cases, an extreme of which is b_e. The average estimate of b will thus be $<b = b_o$.

the size of the interphase nuclei. This correction is only necessary when absolute values are needed. In many situations relative values will suffice and these need not be corrected.

There have been few actual measurements of this correction factor which is influenced by additional elements such as the oval shape and size of the mitotic figures and interphase nuclei, the plane of the section and the section thickness. These, on the whole, have not been considered in the past and other undefined factors may also be involved. We suggest a slightly refined formula and have measured this geometric correction factor and discussed its use. We also show that a correction factor can be deduced directly from measurements of the mitotic index (MI) in whole crypts and sections, which makes no assumptions about the processes involved, and from mitotic accumulation studies using computer modelling techniques, as described in an accompanying paper (Loeffler *et al.*, 1988).

MATERIALS AND METHODS

Animals

Male B6D2F1 (Pat) mice were used between the ages of 10 and 12 weeks when they weighed approximately 25 g. The animals were bred and housed under conventional conditions and received food and water *ad libitum*.

Sampling times and treatment groups

For each sample in the present study, groups of 4 mice were used. Groups of animals were killed at various times of the day from 03·00 to 21·00 h. In some groups the animals received 0·925 MBq (25 μCi) of tritiated thymidine 40 min before killing. In other groups, animals received 0·02 mg of vincristine sulphate (Oncovin, Lilly, Basingstoke) 1, 2 or 3 h before killing. This dose is approximately equal to 0·8 mg/kg which is on the peak of the mitotic arrest *versus* dose curve (Tannock, 1967). The ileum was removed for fixation.

Histology

Some ileal samples were fixed in Carnoy's fixative prior to processing for routine paraffin histology in which case 10 samples were bundled together in tape, sections were cut at 3 μm and stained with haematoxylin and eosin as described elsewhere (Potten & Hendry, 1985).

Other ileal samples were fixed in 10% formal saline prior to processing for resin (hydroxypropyl methacrylate) embedding and sectioning. Sections were cut at approximately 1 μm thickness and were stained in Masson's trichrome, haematoxylin or PAS.

Some tissue was fixed flat (after slitting open the intestine) embedded in either resin or paraffin and sectioned to provide cross sections of the crypt–crypt transverse sections. Some Carnoy-fixed samples were hydrolysed, stained with Schiff's reagent and whole crypts were isolated according to the method of Wimber *et al.* (1960). The whole crypts were placed on a microscope slide in 45% acetic acid and the preparation was viewed and scored immediately in an unsquashed state. The number of mitotic figures and the total cells per crypt were counted by focusing through the crypt (optical sectioning) (Fig. 2). The point at which the crypts break from the villus is beyond precise control but the data suggest that it is fairly uniform and close to the crypt–villus junction as determined subjectively from sections.

Scoring procedures

For the 3 μm paraffin sections one side (half) of 100 good longitudinal crypt sections were scored per mouse. Sections of crypts were selected only if they included both Paneth cells, some evidence of the lumen and at least 17 nuclei along the side of the crypt. Counting was continued along the selected crypt columns until the top of the crypt (the crypt–villus junction) was reached. This provided a value for the average length of a crypt column. The number and position of every mitotic cell was recorded in 100 half-crypt sections from each of 4 mice. Adjacent half-crypt sections were generally from the same crypt. From this an average value for the number of mitotic cells per half-crypt section was determined. This was doubled to give the value per crypt section. For the whole crypts the number of mitotic figures in 50 crypts from each of 4 mice was determined by focusing fully through each whole crypt.

In both the paraffin sections and the whole crypts the mitotic figures were categorized into their respective phases of mitosis. The orientation of the metaphase plates and the anaphase polarity were also recorded in relation to the long axis of the crypt.

Measurements of cell and crypt dimensions

Using both 3 μm paraffin and 1 μm resin sections of the ileum individual crypt sections were selected and photographed using a ×40 planapochromat oil immersion Zeiss lens at a magnification of about ×250. Both longitudinal and transverse crypt sections were used. The photographs were enlarged by a further ×7 (i.e. total magnification of ×1750). A stage micrometer was photographed at the same time. Measurements were then made on these photographs. The number of individual measurements varied depending on the parameter being studied and is shown in the various tables of results. For the most critical measurements

100 cells or crypts were analysed from sections of 4 mice. Mean values were calculated and these are presented in tabular form or as frequency distributions.

RESULTS

Data

Table 1 compares the total number of mitotic figures seen in whole crypts dissected from the intestine with the number seen in good longitudinal 3 μm sections of the crypt (transverse sections of the intestine). About one-third of the total number of mitotic figures seen in a whole crypt are detected in longitudinal sections. This factor of 2·9 is thus the correction required when the number of mitotic figures per crypt section is to be converted to give the total mitotic figures per crypt. Table 1 also shows the total number of epithelial cells per crypt section and the total number of cells in the whole crypt. The ratio of these two values (235/43·8) is 5·4, i.e. one-fifth of all the cells per crypt are seen in a good longitudinal section. These figures can also be used to provide mitotic indices for the whole crypt (MI_c) 4·4/235 = 0·019 and for a crypt section (MI_s) 1·4/43·8 = 0·032. Table 1 also provides evidence for the slight circadian rhythm in mitotic

Table 1. Mitotic figures and cells per crypt and per crypt section

	Isolated intact crypts		Sections of crypts		
Time of day of treatment	Cells per whole crypt*	Mitotic figures per whole crypt	Mitotic figures per longitudinal 3 μm section (whole crypt)	Cells per crypt column (half crypt)†	Ratio of mitotic figures in crypt to section
09.00	217	4·1	1·4	22	2·9
15.00	—	4·2	1·4	22	3·0
15.00	244	4·6	1·4	23	3·4
18.00	—	3·4	1·3	21	2·0
21.00	—	4·1	1·5	21	2·7
03.00	244	4·4	1·4	—	3·1
03.00	—	4·4	1·5	21	2·9
06.00	—	5·6	1·5	23	3·7
Mean	235	4·4	1·4	21·9†	2·9
15.00					
VCR 1 h		8·6	2·8	—	3·1
2 h		16·5	4·5	—	3·7
3 h		20·3	4·9	—	4·2
03.00					
VCR 1 h		11·0	3·1	—	3·5
2 h		17·4	5·2	—	3·4
3 h		25·9	8·2	—	3·2
					Mean 3·5
					Overall mean 3·2

Four mice per group. One-third of all mitotic figures per crypt are seen in good longitudinal sections. VCR, vincristine 0·02 mg per mouse.

* Mean value of 4 mice with 25 crypts counted per mouse.

† Number of cell positions to the crypt–villus junction subjectively determined on 50 sections per mouse and 4 mice per group. The number of cells per crypt section will be twice this value, i.e. 43·8. There are about 18·3 cells per crypt circumference (see Table 3).

activity. Depending somewhat on the time of day the slopes of the mitotic accumulation data suggest that between 5·9 ± 1·2 and 7·5 ± 0·6 cells enter mitosis/h/crypt (15·00 and 03·00 h data respectively). Table 2 shows that up to about four to seven times more mitotic figures have their spindle axis parallel with the long axis of the crypt. Thus, many more full metaphase plates are seen in transverse sections of the crypt and more bipolar anaphase figures are seen in longitudinal sections.

Table 2. Orientation of mitotic figures in 3 μm paraffin sections

	Sections				Whole crypts†	
	Longitudinal (L) crypt sections (%)*	Transverse (T) crypt sections (%)	Ratio T:L		%	Ratio H:V
Prophase	33·3	39·2	1·2:1		—	
Metaphase						
side view	22·7‡	3·3§	1:6·9	Side view vertical (V)	3·1§	
end view (full plate)	7·4§	42·4‡	5·7:1	Side view horizontal (H)	16·2‡	5·2:1
Anaphase	18·1‡	7·1§	1:2·5		—	
Anaphase and telophase	23·3‡	10·7§	1:2·2¶	Horizontal	2·9§	
				Vertical	12·3‡	1:4·2

Up to six to seven times more mitotic figures are orientated with the poles of the spindle parallel to the long axis of the crypt. Thus more anaphases are seen in longitudinal sections and more full metaphase plates in transverse sections.

* Percentage of 1000 mitotic figures counted. Includes about 15% mitotic figures that could not be reliably assigned to the phases.

† Of 800 mitotic figures.

‡ Indicates a vertical mitotic pole (parallel to crypt long axis).

§ Indicates a horizontal mitotic pole (circumferential axis).

¶ The same ratio also obtained in another experiment.

Table 3 shows the physical dimensions of the crypts as seen in longitudinal and transverse sections of the crypts. The crypts are about 25% narrower at the top near the villus. They also appear to be narrower (20%) when measured from 3 μm paraffin sections, possibly because of differences in tissue shrinkage. There is about a 10% shrinkage in the diameter after 3 h mitotic accumulation after vincristine treatment which is probably the consequence of the reduction in the number of cells per crypt, because emigration continues but cell production is stopped. Somewhat surprisingly, there is an expansion by about 25% in the crypt diameter when the measurements are made on transverse crypt sections. This may be because some oblique sections are inevitably measured and also because there is a relaxation of the tension within the tissue when the intestine is slit open and the intestinal muscles are cut prior to the fixation for this type of sectioning. However, in contrast, the diameter of the crypt in longitudinal sections will be slightly underestimated because of some non-axial sections (see Fig. 3).

Table 4 illustrates the fact that the interphase nuclei are approximately flattened spheres in shape with a diameter that is about 25% greater when seen in transverse sections of the crypt. This can be clearly seen in Figs 1 and 2. The average diameter of a mitotic figure is 10% smaller than that of an interphase nucleus. Although a mitotic cell is undoubtedly larger than an interphase cell the nuclear material is more condensed and it is this which is recognized as a mitotic figure. The frequency distributions for the radii of mitotic and interphase cells measured

Table 3. Diameter of crypts

	Diameter from centre of epithelial nuclei (μm)	Radius (μm)	Total diameter to outer edge of nuclei (μm)	Lumenal diameter (μm)*
Longitudinal 1 μm crypt sections				
overall	30·88 (50) (18·3 cells)‡	15·44	36·22	<4·99
base only	35·62 (14) (19·5 cells)‡	17·81	—	—
top only	26·70 (15) (17·0 cells)‡	13·35	—	—
Longitudinal 3 μm crypt sections	24·50 (54)	12·25	31·22	—
Longitudinal 3 μm crypt sections (3 h VCR)	21·83 (146)	10·91	—	—
Transverse 1 μm crypt sections	40·02 (45)†	20·01	46·74	<3·91

* Upper limit since crypts with a very small or closed lumen would not be counted.

† May be larger because of some oblique sections and a relaxation or loss of tension because the circumferential muscles have been severed before fixation.

‡ Number of cells per circumference determined from 200 crypt sections from 4 mice.

Number of measurements shown in parentheses. See Fig. 5 for an example of the full distribution of values. VCR, vincristine.

Table 4. Nuclear sizes

	Interphase nuclei radius (μm)	Mitotic figures radius (μm)
Longitudinal 1 μm crypt sections	2·76† (61) 3·39‡ (61) (r_N)	2·47 (61)
Prophases	—	2·21 (12)
Anaphases	—	3·26 (6)
Base of crypt	2·76† (15)	2·67 (16)
Top of crypt	2·51† (16)	2·21 (16)
Transverse 1 μm crypt sections*	3·38 (100) (r_N)	2·98 (100) (r_M)
Prophases	—	2·91 (15)
Anaphases	—	3·18 (7)

* Some oblique sections may be scored and there may be a relaxation or loss of tension because the circumferential muscles have been severed before fixation.

† Mean of long and short axis measurements.

‡ Mean of long axis measurements (equivalent to transverse section measurements).

The nuclei are about 20% larger in diameter in transverse sections. The diameter in transverse sections determines the probability of appearance in longitudinal sections. Mitotic figures are about 10% smaller than the interphase nuclei.

See Fig. 4 for an example of the full distribution of values. Number of measurements shown in parentheses.

from 1μm transverse sections are shown in Fig. 4. Although the width of the crypt (radial measurements) is influenced by the muscular tension at fixation the shape of the cell nuclei does not appear to be influenced.

Table 5 shows the radial position of mitotic figures and interphase nuclei measured at the

respective diameters can be easily measured on such transverse sections as was implied by Tannock (1967). However, since MI's are actually measured on longitudinal sections and the preparation of transverse sections may result in some tissue architecture distortion (see Table 3) the measurement should be conducted on longitudinal sections. However, the diameter of the mitotic figures and interphase nuclei should in principle be determined on sections at right angles to the sections used for counting, i.e. should be made on the transverse sections. The interphase nuclei have a flattened sphere shape, such that the diameter of the sphere is best measured in transverse crypt sections. However, a reasonable measure of this diameter may also be obtained from the longer of the two nuclear diameter measurements seen in longitudinal sections (see Table 4). The factor by which MI data obtained from longitudinal crypt sections should be corrected when geometric considerations are taken into account (*f* Tannock, abbreviated to f_T) can be defined as follows (modified according to Tannock, 1967 and Wright & Alison, 1984):

$$f_T = \frac{a_o}{b_o} \cdot \frac{T + 2(r_N - K)}{T + 2(r_M - K)}$$

where a_o is the average radial position of the centre of mitotic figures in longitudinal sections and r_M is the average radius of mitotic figures measured either at right angles, i.e. in transverse sections or from the long axis of the mitotic figures in longitudinal sections, b_o is the radius of the crypt (to the centre of the interphase nuclei in longitudinal sections) and r_N is the average radius of interphase nuclei in transverse sections or from the long axis of the nuclei in longitudinal sections. T is the section thickness (3 μm here) and K the diameter of the smallest recognizable fragment (0·5 μm assumed here).

The radii a_o and b_o are those as measured in longitudinal sections, and will differ from the true radii a and b as some sections will not be truly along the axis of the crypt (Fig. 3). Tannock (1967) suggested that the true radii a and b be used, which overestimates the correction factor if experimentally one includes some non-axial sections ($a_o/b_o \leqslant a/b$). In practice, a more detailed mathematical treatment showed that the use of a_o/b_o rather than a/b corrects for this overestimation since various elements cancel each other out.

When the radial positions of mitotic and non-mitotic cells are taken from 3 μm longitudinal sections and the nuclear radii are taken from transverse sections we have:

$$f_T = \frac{6{\cdot}03}{12{\cdot}64} \cdot \frac{3 + 2\,(3{\cdot}38 - 0{\cdot}5)}{3 + 2\,(2{\cdot}98 - 0{\cdot}5)} = 0{\cdot}53$$

If all measurements are made on 1 μm sections a value of 0·56 is obtained and if all measurements are taken from transverse sections a value of 0·65 is obtained. Although this latter is the approach adopted by Tannock (1967), we believe that measurements made on both longitudinal and transverse sections as outlined above are more appropriate, i.e. a correction factor $f_T = 0{\cdot}53$. These figures are presented to show that the geometric correction factors can differ by up to about 20% depending on how they are estimated. This variation should be considered in relation to the overall experimental variances.

Modelling procedure using mitotic accumulation data

We have recently presented a computer model of cell replacement in the crypt (Loeffler *et al.*, 1986) which could also be used to analyse MI data as presented in the accompanying paper (Loeffler *et al.*, 1988). Fitting model simulations for mitotic arrest to actual vincristine mitotic accumulation data produced estimates for the mitotic phase duration (T_M) and for the geometrical correction factor. The correction factor f_{mod} occurs because the model does not allow

for the centripetal positioning of mitotic cells. Consequently if mitotic accumulation experiments are simulated, the model will systematically generate fewer mitoses than seen in actual crypt sections at identical time points. This discrepancy is overcome by introducing a specific model simulation time 't_{sim}' which runs faster than the chronological time 't' by a certain factor which is f_{mod}. The M phase duration in the simulations also has to be rescaled by f_{mod}.

Thus, we equate the MI obtained in sections in vincristine (VCR) accumulation experiments with a model-derived MI,

$$MI_{s,exp}\ (t) = MI_{s,mod}\ (t_{sim}) \text{ leading to the equation}$$

$$(T_M + t - t_o) = (T_{M,sim} + t_{sim}) \times f_{mod}$$

t being the chronological time after VCR and t_0 the time lag before VCR takes effect, taken to be 0·5 h (based on other VCR studies, Chwalinski & Potten, 1986 and Al-Dewachi *et al.*, 1975 who determined it to be 20 min).

The model is best fitted (by least squares) to all the VCR data in a 3 h accumulation experiment with $T_{M,sim} = 1$ h and $t_{sim} + t_o = 4{\cdot}25$ h. Using these values one can derive estimates for T_M and f_{mod} by evaluating, e.g. the 0·5 h and 3 h time points:

$$0{\cdot}5 \text{ h VCR: } t - t_o = t_{sim} = 0\text{: } T_M = 1 \text{ h}.f_{mod}$$

$$3 \text{ h VCR: } t - t_o = 2{\cdot}5,\ t_{sim} = 3{\cdot}75\text{: } (T_M + 3 \text{ h} - 0{\cdot}5 \text{ h}) = (1 \text{ h} + 3{\cdot}75 \text{ h}).f_{mod}$$

Solving these two equations gives $T_M = 0{\cdot}66$ h and $f_{mod} = 0{\cdot}66$.

The correction factors discussed above are summarized in Table 6 including the simple ratio a/b which Tannock adopted. Considering the section thickness and nuclear diameters raises the ratio a/b by about a factor of 1·1.

Table 6. Correction factors

Technique	Sections/whole crypts ratio	$a_0 b_0$ (Table 5)	f_T	f_D	f_{mod}
Longitudinal 1 μm sections	—	0·50	0·56	—	—
3 μm sections	—	0·48	0·53	—	—
3 μm sections (VCR)	—	0·48	—	—	—
Transverse 1 μm sections	—	0·60	0·65	—	—
Longitudinal 3 μm sections					
mitotic cells	2·9*	—	—	0·59	—
total cells	5·5*†				
Computer modelling of crypt after mitotic arrest	—	—	—	—	0·66

* Factor by which whole section counts have to be multiplied to give data for the whole crypt.

† Morphometric calculations (number of columns × count) should be multiplied by 0·6 to give actual values as determined from whole crypts.

VCR, vincristine.

If a geometric correction factor is required we believe it should take section thickness and nuclear diameter into account and should be measured on longitudinal paraffin sections. However, this is unlikely to take into account all considerations. f_D and f_{mod}, which we believe to be equivalent and all-encompassing and hence should be used, are 20% greater than the geometric factor f_T. Fortuitously, the geometric factor using radii measured on transverse sections gives a value virtually identical to f_D.

DISCUSSION

The reasons why the mitotic figures are displaced centripetally remains obscure but it has been suggested that this may facilitate the determination of the repositioning of the two daughter cells back into line with the non-mitotic cells (Loeffler *et al.*, 1986; Potten & Loeffler, 1987). The significance of the polarity of mitotic figures is also unclear. At metaphase most (75–85%) of the mitotic figures have their poles arranged vertically, as also described elsewhere (Lamprecht *et al.*, 1986). The reason why the anaphase polarity is less striking is probably because of difficulties in reliably identifying anaphase figures, particularly when only one pole may be present. The polarity of anaphase figures is better viewed in whole crypts (Table 2). Once the new daughter cells are re-insinuated into the crypt wall a greater proportion (40–80%) of the two daughter cells are believed to end up lying next to each other (i.e. within the circumference) than on top of each other (i.e. in the vertical column of cells) (Loeffler *et al.*, 1986; Potten & Loeffler, 1987). Lamprecht *et al.* (1986) also concluded that there was "no correlation between the orientation of the mitotic spindle and the direction of epithelial cell migration" based on morphometric studies.

The value of 235 cells per crypt is only slightly lower than a previous estimate from our laboratory (Kovacs & Potten, 1973). In unpublished serial reconstruction studies performed on two crypts we obtained 230 cells, five of which were mitotic, and 226 cells, three of which were mitotic. These values support our assumption that the data presented in Table 1 for whole crypts are the most realistic representation of the cellularity and mitotic activity of crypts.

Tannock (1967) reported a value of 0·57 for the geometric correction factor for the jejunum in Marshall rats. Wright, Morley & Appleton (1972) presented a value of 0·62 for the jejunum of Wistar rats while Sunter *et al.* (1979) presented four values for different areas in the large bowel of mice, the mean value of which was 0·58. Al-Dewachi *et al.* (1975) presented a value of 0·73 for mouse jejunum but the precise details of how this was derived were not presented. The present studies would suggest a value of 0·59 if determined directly by scoring mitotic figures and interphase nuclei in whole crypts and comparing these with data from sections (f_D) or a geometric factor (f_T) of 0·53–0·56 if determined on longitudinal sections.

However, we feel that there are a number of ambiguities in connection with this type of calculation. (1) There is some confusion as to whether the measurements should be made on transverse or longitudinal sections. The longitudinal sections may tend to underestimate the radii due to non-axial sections while the transverse sections would tend to overestimate the radii due to tissue relaxation and oblique sections. There was no indication in the present studies that these measurements varied with cell position. (2) Section thickness influences the ratio of nuclear to mitotic diameters. The section thickness is difficult to define and control precisely. However, the influence of section thickness is small over the range 1–10 μm. (3) The nuclei are, on the whole, flattened spheres with their thin cross section being evident in longitudinal sections of the crypt. The shape of the nuclei may vary somewhat and there is some confusion as to which dimension to consider. (4) The minimum size of a nuclear or mitotic slice that can be recognized is unknown and probably differs between mitotic and interphase nuclei and between observers. (5) The sizes and identification ability for prophases, metaphases, anaphases and telophases may vary between observers.

For these reasons we feel that the direct correction factor (f_D) has less uncertainties and ambiguities and so should be adopted.

Calculation of the error limits on the various factors would be mathematically complex and would involve a number of further assumptions. Approximate estimates indicate that the errors will not be more than $\pm 20\%$.

We have recently presented a computer model of the crypt (Loeffler *et al.*, 1986) where we have a rectangular lattice of 16 cells in circumference and 24 cells per crypt column. This gives a crypt of 384 cells. Actual measurements on transverse and longitudinal crypt sections shows 18·3 cells per circumference and 21·9 cells per column. These would give a crypt of 400 cells — very similar to the model. Actual measurements from unsquashed whole crypts gave a value of about 235 cells (Table 1) which is consistent with a crypt of 15·5 × 15·5 cells. Thus the model and morphometric calculations both contain 1·6–1·5 times too many cells, i.e. the number of cells in each case should be multiplied by a factor of 0·6. The number of cells seen in a longitudinal crypt section will depend on the shape and packing of cells. Counts on whole intact crypts suggest that there are really 15–16 cells up the sides of a crypt, i.e. that the sections usually showing 22 positions overestimate the true number of cells by about 1·4 or should be multiplied by a factor of 0·7. The model overestimates the cell positions and total cells per crypt by about the same amount and hence gives a very good representation of the labelling or MI data derived from sections. We believe these effects are more to do with the polygonal packing arrangements than with the problems associated with overlapping nuclear profiles which were discussed by Clarke (1975). The points outlined here explain the differences seen between the estimates for total cells per crypt based on the whole crypt counts and those obtained by morphometric considerations (see Al-Dewachi *et al.*, 1975).

The longitudinal sections overestimate the cell count by about 40%. This is almost the same factor (30%, Table 4) by which the nuclei are flattened, i.e. the long axis of the nucleus is 30% greater than the short axis. This could all be understood if the cells were packed in such a way as to present a hexagonal profile at the surface wall of the crypt, as is suggested in part by scanning electron microscopy of the villus surface, with the major hexagon overlaps in the longitudinal plane.

ACKNOWLEDGMENTS

This work has been supported by the Cancer Research Campaign UK. Over the years a number of people have been involved with these, and related experiments. However, we are particularly grateful to Caroline Chadwick, Gary Owen, Paula Jones and Helen Moffatt.

REFERENCES

AL-DEWACHI, H.S., WRIGHT, N.A., APPLETON, D.R. & WATSON, A.J. (1975) Cell population kinetics in the mouse jejunal crypt. *Virchows Arch. B [Cell Pathol.]* **18**, 225.

CHWALINSKI, S. & POTTEN, C.S. (1986) Radiation-induced mitotic delay: duration, dose and cell position dependence in the crypts of the small intestine in the mouse. *Int. J. Radiat. Biol.* **49**, 809.

CLARKE, R.M. (1975) The effect of intestinal distension and of section thickness on counts of epithelial nuclei in the rat small intestine. *J. Microsc.* **103**, 333.

KOVACS, L. & POTTEN, C.S. (1973) An estimation of proliferative population size in stomach, jejunum and colon of DBA-2 mice. *Cell Tissue Kinet.* **6**, 125.

LAMPRECHT, J., ZIEBA, P. & STROJNG, P. (1986) Spatial orientation of the mitotic apparatus and its stability in a polarised epithelial cell. A computer-assisted morphometric analysis. *Anat. Embryol.* **175**, 129.

LOEFFLER, M., POTTEN, C.S., PAULUS, U., GLATZER, J. & CHWALINSKI, S. (1988) Intestinal crypt proliferation. II. Computer modelling of mitotic index data provides further evidence for lateral and vertical cell migration in the absence of mitotic activity. *Cell Tissue Kinet.* **21**, 247.

LOEFFLER, M., STEIN, R., WICHMANN, H.E., POTTEN, C.S., KAUR, P. & CHWALINSKI, S. (1986) Intestinal cell proliferation I. A comprehensive model of steady-state proliferation in the crypt. *Cell Tissue Kinet.* **19**, 627.

POTTEN, C.S. & HENDRY, J.H. (1985) The micro-colony assay in mouse small intestine. In *Cell Clones: Manual of Mammalian Cell Techniques* (Ed. by Potten, C.S. & Hendry, J.H.), p. 50. Churchill-Livingstone, Edinburgh.

POTTEN, C.S. & LOEFFLER, M. (1987) A comprehensive model of the crypts of the small intestine of the mouse provides insight into the mechanisms of cell migration and the proliferation hierarchy. *J. Theoret. Biol.* **127**, 381.

SUNTER, J.P., APPLETON, D.R., DE RODRIQUEZ, M.S.B., WRIGHT, N.A. & WATSON, A.J. (1979) A comparison of cell proliferation at different sites within the large bowel of the mouse. *J. Anat.* **129**, 833.

TANNOCK, I.F. (1976) A comparison of the relative efficiencies of various metaphases arrest agents. *Exp. Cell Res.* **47**, 345.

WIMBER, D.E., QUASTLER, H., STEIN, O.L. & WIMBER, D.L. (1960) Analysis of tritium incorporated into individual cells by autoradiography of squash preparations. *J. Biophys. Biochem. Cytol.* **8**, 327.

WRIGHT, N.A., MORLEY, A. & APPLETON, D. (1972) Variation in the duration of mitosis in the crypts of Lieberkhun of the rat: a cytokinetic study using vincristine. *Cell Tissue Kinet.* **5**, 351.

WRIGHT, N.A. & ALISON, M. (1984) *The Biology of Epithelial Cell Populations.* Clarendon Press, Oxford.